ISSN (Online) 2394-2320

International Journal of Engineering Research in Computer Science and Engineering (IJERCSE)

Vol 10, Issue 01, January 2023

Breast Tumour Detection using Deep Convolutional Neural Networks

[1]Himashri Mehra, [2]Anushka Singhania, [3]Anu Narera, [4]Neha Singh

[1][2][3][4] Indira Gandhi Delhi Technical University for Women, New Delhi, India
Email: [1] himashri050btece19@igdtuw.ac.in, [2] anushka071btece19@igdtuw.ac.in, [3]anu048btece19@igdtuw.ac.in, [4] nehasigdtuw@gmail.com

***Abstract*— Breast cancer is one of the most fatal cancers for women. Because of its high mortality rate, it is becoming a necessity for the researchers to come up with models for precise detection of disease and subsequent treatments. By doing this, the researchers will not only promote the new technology but also contribute to the mankind. We are also trying to do the same. This paper proposes the semantic image segmentation of breast tumour using ResUNet model. The proposed model attained a high accuracy of 0.9871 on our training dataset. The complete empirical analysis along with the exhaustive literature review is presented in the paper.**

***Keywords*— Breast Tumour, ResUNet, Semantic Image Segmentation, U-Net**

I. INTRODUCTION

Worldwide cancer ranks foremost reason for death before the age of 70 years across 91 out of 172 nations. As stated in the GLOBOCAN report of 2018, 9.6 million deaths were documented and 18.1 million new cancer patients were reported globally. The 2018 report on medical certification reveals cancer as the fifth prominent reason of death by estimating 5.7% of all deaths in India [1]. In India, GLOBOCAN data 2020, breast cancer accounted for 13.5% of all cancer cases and an estimated 10.6% of all deaths with a cumulative risk of 2.81% [2]. There is a rapid upsurge in breast cancer cases both in rural and urban areas. Survival rates of cancer patients decline with the higher stages of cancer growth. In India, stage 3 and stage 4 breast cancer affects more than 50% of female patients. According to statistics, Indian women had a 60% post-breast cancer survival rate compared to an 80% rate in the USA. The younger age group is reported to have a higher incidence of breast cancer. Moderately 50% of all cases are in the 25-50 demographic range. The above-cited concern depicts the lack of awareness among the masses which led to delays in diagnosis and higher mortality rates. Another prominent reason for the low breast cancer survival rate is low-grade early screening and diagnosis rates. The efficiency of screening programs relies on considerable elements and one of them is a fitting instrument for diagnosis to accurate execution. That can be accomplished by the application of data science methods in image processing as image segmentation.

II. LITERATURE REVIEW

One of the utmost perplexing problems in medical image analysis is distinguishing the pixels of organs or lesions from background medical pictures like CT, MRI, or Ultrasound Images in order to provide essential information on the shapes and volumes of these organs. Hesamian et al. [3] proposed models that have been examined over the years that presented diverse automated segmentation systems by applying available technologies. The exemplified approach encloses Convolution Neural Network (CNN), 2D CNN, 2.5 CNN, 3D CNN, Fully Convolution Neural Network (FCN), Cascaded FCN (CFCN), FCN for multi-organ segmentation, Multi-stream FCN, U-Net, V-Net, Convolutional Residual Networks (CRNs), Recurrent Neural Networks (RNNs) that have utilised deep-learning techniques for medical image segmentation. Deeper networks are proven to have adequate performance regardless there are some challenges in conditioning deep models like overfitting, training time, gradient vanishing, and 3D challenges.

For the categorization of breast ultrasound images, Inan et al. [4] constructed an end-to-end integrated pipeline and evaluated image pre-processing techniques including K Means++ and SLIC, furthermore four transfer learning models such as VGG16, VGG19, DenseNet121, and ResNet50. The combination of SLIC, U-NET, and VGG16 exceeded all other incorporated sequences by a Dice-coefficient score of 63.4% in the segmentation step and precision and the F1-Score (Benign tumour) of 73.72% and 78.92% in the classification stage. The proposed automated pipeline can be successfully implemented to aid medical practitioners make precise and prompt diagnosis of breast cancer.

Tarighat[5] presented breast tumour segmentation employing a DCNN by U-Net. This postulated U-Net model contains an asymmetric expansion path for precise localization and a contractile path to capture the background, yielding an IOU of 68% and an all-around accuracy of 91%.

Aimed at the objective of segmenting breast mass in full-extent mammograms, Zaho et al. [6] presented an unexplored adaptive channel and multiscale spatial context network. The two open datasets, CBIS-DDSM and INbreast, a ResNet

ISSN (Online) 2394-2320

International Journal of Engineering Research in Computer Science and Engineering (IJERCSE)

Vol 10, Issue 01, January 2023

model and a detailed ACMSC component are incorporated and tested. The network can understand different feature maps because of the ACMSC module's multilevel embedding, which yields 84.11% INbreast and 82.1% CBIS-DDSM of dice coefficients correspondingly.

Anand et al. [7] suggested a ResUNet model for breast tumour segmentation. The suggested framework includes the residual network technique that improves performance and exhibits an enhanced training procedure and implementation of ResUNet, which was examined with conventional U-Net, FCN8, and FCN32. On the MRI dataset, the suggested model's overall accuracy was 85.32%, with a dice coefficient of 73.22%.

A two-stage approach suggested by Wu et al. [8] uses contrast images for the segmentation of breast tumour, constructs the breast ROI, and then directs an attention network to differentiate between carcinogenic regions and healthy breast tissue. The suggested model delivers a compelling cancer segmentation resolution for breast analysis operating DCE-MRI, resulting in a 91.11% Dice coefficient for breast tumour segmentation.

As a means to solve the sparse data reconstruction problem, Zhang et al. [9] introduced a unique DL-MITAT way and used it to identify breast cancer. The system used is the domain transform network termed FPNet + ResUNet. To evaluate the efficacy of the DL-MITAT strategy, ex-vivo and simulation tests using breast phantoms were performed. Generated images give in-depth explanations on the capacity and limitations of the suggested method and are of preferable quality and contain fewer artifacts than those produced by a traditional imaging method.

In order to accurately segment mass lesions in mammogram images, Abdelhafiz et al. [10] suggested a residual attention U-Net model, succeeded by a ResNet classifier to categorise the identified binary segmented lesions either benign or malignant. To retain the more dimensions and contextual data, which helps the network to tackle gradient disappearing challenge and have a multi-layered structure, residual attention modules were introduced to the U-Net model.

III. METHODOLOGY

Flowchart of the proposed methodology is shown in Fig.1.

A. Dataset Description

The dataset, which analyses ultrasound scan images of breast cancer, was obtained from Kaggle [11]. Breast ultrasound images taken among women between the ages of 25 and 75 are part of the preliminary information. In total, there are 600 female patients. The collection consists of 780 photos, each measuring 562 by 471 on average. The images are PNG files. In addition to the original images, ground truth images are also displayed. Three categories - benign, malignant and normal, are further used to group the images.

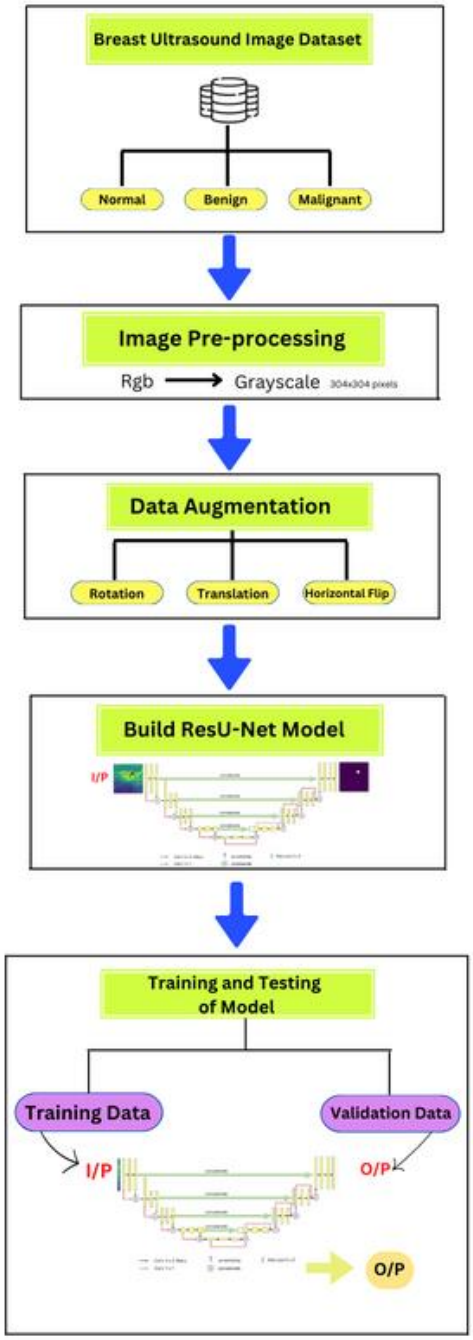

Fig. 1: Flowchart of the proposed methodology

B. Image pre-processing

Since every image in the dataset has a different shape, there is a possibility of occurrence of an error when the images are run through the proposed framework. To address this issue, we converted all of the breast ultrasound images and mask images into (304 x 304) forms. The mask images were converted from RGB format into grayscale to save time. In Fig. 2 and Fig. 3, we can see a set of original and modified images respectively.

ISSN (Online) 2394-2320

International Journal of Engineering Research in Computer Science and Engineering (IJERCSE)

Vol 10, Issue 01, January 2023

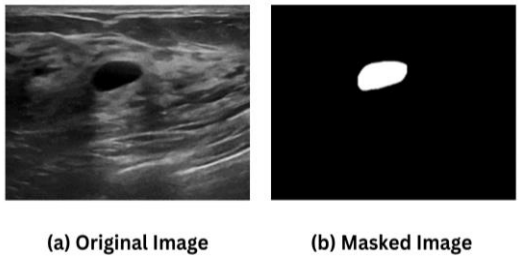

Fig. 2: Original (a) Breast Ultrasound image of size (562 x 471 x 3) and (b) Masked image of size (562 x 471 x 3)

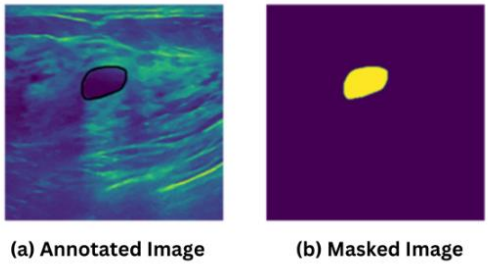

Fig. 3: Modified (a) Annotated Breast Ultrasound image size (304x304x3) and (b) Masked image of size (304x304x1)

C. Data Augmentation

One of the most efficient ways for increasing the amount of dataset is to use the image augmentation technique, which is a method of altering the original images through the application of several transformations, along with the generation of numerous altered versions of the same original image. For the purpose of preventing our proposed method from resulting in a fragile solution that will fail because it was trained only on a small image dataset, augmentation is performed on the dataset so that every single new batch that is passed over to the proposed method observes a slight variation in the dataset each time. Even though the data will change constantly, as a result, this will allow the proposed method to be able to generalise solutions and unseen data effectively. For performing image augmentation, KerasImageDataGenerator class has been applied. The input of the original image data is obtained using the KerasImageDataGenerator, which transforms the input data randomly, and produces a result that solely comprises the newly altered data. With the ImageDataGenerator, two distinct functions were defined: one for the original images and the another one for masked images. For the purpose of increasing the generalisation of the model entirely, data augmentation is carried out using the Keras picture data generator class. Through the image data generator, the data augmentation operations involving rotations, translations, shear in, scale adjustments, and horizontal flips, were performed randomly.[12]

D. Proposed ResUNet approach for Semantic Segmentation

In this study, we propose the Deep Residual U-Net (ResUNet) [13] for semantic segmentation of breast ultrasound images. In view of the advantages of the U-Net [14] architecture and Deep Residual Learning, we have proposed the ResUNet architecture. The architecture of ResUNet combines ResNet [15] architecture's residual block with the U-Net architecture.The residual block, pooling layer, and convolutional layer have all been adjusted. The residual block is included after an up-sampling layer to handle the segmentation of intricate structures and two convolutional layers to regenerate the feature space, prior to fusing the down sampling layer's feature map. The residual block improves the learning effectiveness and even reduces disappearing gradient problems when introduced to the U-Net architecture. It has two distinct branches, namely the trunk branch and the mask branch. The trunk branch comprises the convolution layers, Batch Normalisation processes (BNs), and Rectified Linear units (ReLus). In the absence of the skip association, the residual block is useless. The skip connection and residual block are depicted in Fig.4. Within the mask branch, in order to establish identity mapping, the input and output are connected using the skip connection.

If x denotes the input, a complex mapping function is denoted by $H(x)$ between the input images and the output feature maps, and $F(x)$ denotes the residual training function; we get

$$F(x) \coloneqq H(x) - x \tag{1}$$

which implies $H(x) \coloneqq F(x) + x$ (2)

The residual block is formed by stacking the residual units in a sequential form, with the output of i^{th} layer y_i of the residual unit [16] being defined as:

$$y_i = h(x_i) + F(x_i, W_i)x_{i+1} = f(y_i) \tag{3}$$

Where f denotes the activation function, W_i indicates the weight of the network that needs to be learned. If all the continuous layers are considered, f corresponds to identity mapping, where, $x_{i+1} \equiv y_i$, then we have

$$x_I = x_i + \sum_{i=1}^{I-1} F(x_i, W_i) \tag{4}$$

Using the back propagation rule, the gradient of (4) can be calculated:

$$\frac{\partial \epsilon}{\partial x_i} = \frac{\partial \epsilon}{\partial x_I}\frac{\partial x_I}{\partial x_i} = \frac{\partial \epsilon}{\partial x_I}\left(1 + \frac{\partial}{\partial x_I}\sum_{j=i}^{I-1} F(x_j, W_j)\right) \tag{5}$$

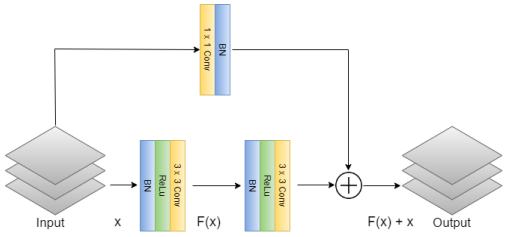

Fig. 4: Skip connection and residual block

ISSN (Online) 2394-2320

International Journal of Engineering Research in Computer Science and Engineering (IJERCSE)

Vol 10, Issue 01, January 2023

The gradient $\frac{\partial \epsilon}{\partial x_i}$ will never be zero if the term $\frac{\partial}{\partial x_I}\sum_{j=i}^{I-1} F(x_j, W_j)$ is not −1, which in practical terms, cannot always be -1 for every sample in a small batch. This makes sure that while the network is being trained; the gradient always runs smoothly and disappears less frequently.

In the residual block, the tensor size undergoes no change. To ensure computational performance, the ResUNet has a consistent number of convolutional layers throughout all the residual blocks.

For this study, the feature map before and after the convolution are combined, in order to effectively combine the overall image features with its intrinsic features. The output of convolution utilizes the feature maps from the two components of concatenate after the feature maps have been combined. Convolutions are used in this procedure to obtain high dimensional features while preserving the initial dimensional features, hence, effectively fusing features at various scales and confirming accurate segmentation.

The dimensions of the feature map and the amount of convolution filters are increased by a factor of two each time the feature map is applied to a residual unit. For confirming that forward processing is generated on the same gradient as the maximum, the data are batch normalised at every residual unit. The proportion of sample data utilised in the backward computation will also be similar to that of the forward computation. This produces a uniform distribution, enables significant adjustments in weight, and prevents the issue of disappearing and exploding gradients during training.

E. Model Architecture and Training

Fig. 5 illustrates the entire system architecture of the proposed ResUNet model. Each convolutional block throughout the network's encoding unit is made up of Recurrent Convolutional Layers (RCLs), to which 3 x 3 convolutional filters are incorporated. These are accompanied by batch normalisation layers, which are preceded by ReLU activation layers. With the support of the activation layer ReLu, the sparse model is able to more effectively extract pertinent features and fit the data for training to enhance the convergence of network. A 1 x 1 convolutional layer is applied in between each of the convolutional blocks for downsampling, followed by a 2 x 2 Max Pooling layer.Each convolutional block in the decoding unit is composed of three types of layers in total, consisting of a concatenation layer, a convolutional transpose layer and two convolutional layers. Then, using 1 x 1 convolutional filters and a sigmoid activation function, the features are projected to the feature map for output. The parameter threshold (T) is empirically adjusted at 0.5 to form the segmented region. The training involves the validation of 10% of the sample data. We keep track of the losses during evaluation and set the patience as 10. The batch size is specified as 6, owing to the physical memory limitations of the GPU. The Adam optimizer [17] is for training the model and the learning rate is set as 1 x 10^4.

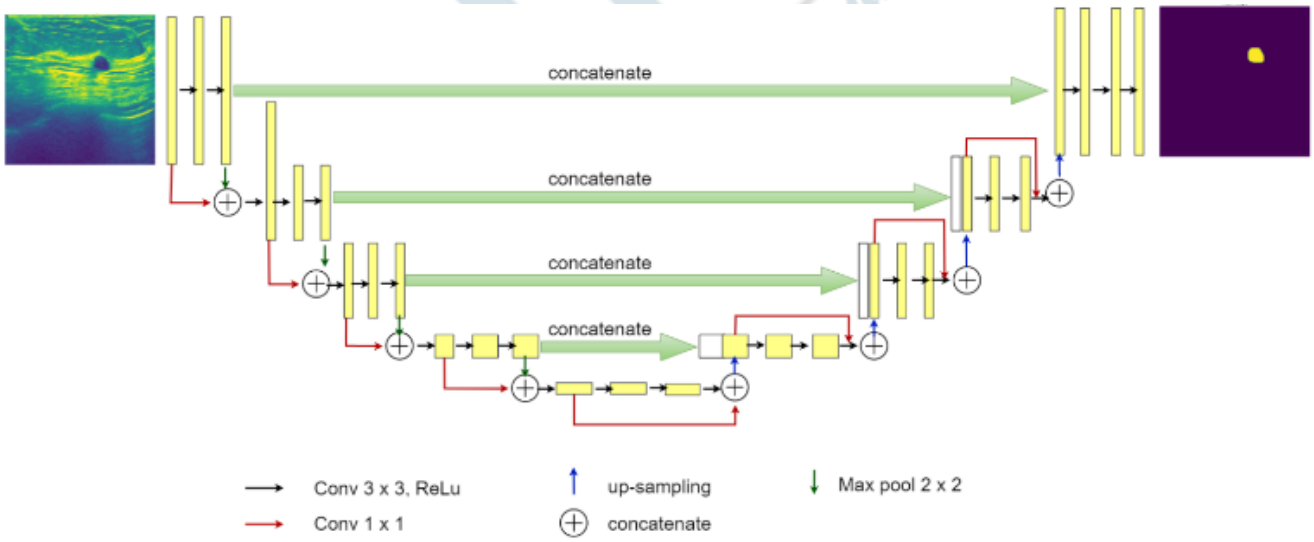

Fig. 5: ResUNet Architecture

F. Evaluation Metrics

A variety of metrics are taken into consideration for conducting the quantitative analysis of the experiment, including Binary Cross Entropy Loss (log loss), accuracy (AC), dice coefficient (DC), specificity (SP) and sensitivity (SE), Area Under the Curve (AUC) and Receiver Operating Characteristics (ROC) curve. Semantic segmentation aims to predict whether pixels in an image belong to an object or not. As a result, this problem can also be described as a pixel-by-pixel binary classifier problem. Therefore, for both training and validation, the loss function based on Binary Cross Entropy is used. If the prediction of model for an input image, is taken as z and its ground truth is y, then the Binary Cross Entropy or log loss J for a batch of n images is as follows:

ISSN (Online) 2394-2320

International Journal of Engineering Research in Computer Science and Engineering (IJERCSE)

Vol 10, Issue 01, January 2023

$$J = \frac{1}{n}\sum_{i=1}^{n} -(y_i \log z_i + (1 - y_i) \log(1 - z_i)) \quad (6)$$

The accuracy and sensitivity are calculated using (7) and (8) respectively.

$$AC = \frac{TP+TN}{TP+TN+FP+FN} \quad (7)$$

$$SE = \frac{TP}{TP+FN} \quad (8)$$

Moreover, specificity can be calculated using (9).

$$SP = \frac{TN}{TN+FP} \quad (9)$$

Where TP indicates True Positive, TN refers to True Negative; FP and FN refer to False Positive and False Negative respectively.

According to [18], DC is stated in (10). The terms "ground truth" (GT) and "segmentation result" (SR) are used here.

$$DC = 2|GT \cap SR||GT| + |SR| \quad (10)$$

IV. RESULTS ADND DISCUSSION

Table I shows the experiment results for both U-Net and the proposed ResUNet. The proposed ResUNet model observes an accuracy of 0.9871, which exhibits an improvement over the accuracy of U-Net, which is 0.9703, by 1.73%. Similarly, the values observed for sensitivity and specificity by ResUNet are higher than that of U-Net. ResUNet observes a much higher AUC, which is 0.9688, 50.41% higher than that of U-Net. In addition, for ResUNet, the average DC calculated in the validation phase is 0.4352, which is significantly better in comparison with U-Net. The log loss obtained for ResUNet is considerably less than that for U-Net.

For qualitative analysis, the overall segmentation results obtained by U-Net and the proposed ResUNet are shown in Fig. 6 and Fig. 7 respectively. The input images are displayed in the first column, the ground truth in the second, the predicted outcome in the third, and the predicted binary outcome in the fourth. In most of the segmentation results generated by ResUNet, with nearly the same shape as the ground truth, the targeted lesions are satisfactorily segmented.

TABLE I: Experimental results of U-Net and ResUNet for Breast Ultrasound Images Semantic Segmentation

Metrics	Model	
	U-Net	ResUNet
Log loss	0.4351	0.0350
AC	0.9703	0.9871
AUC	0.6441	0.9688
SE	0.6863	0.9763
SP	0.6444	0.9999
DC	0.0494	0.4352

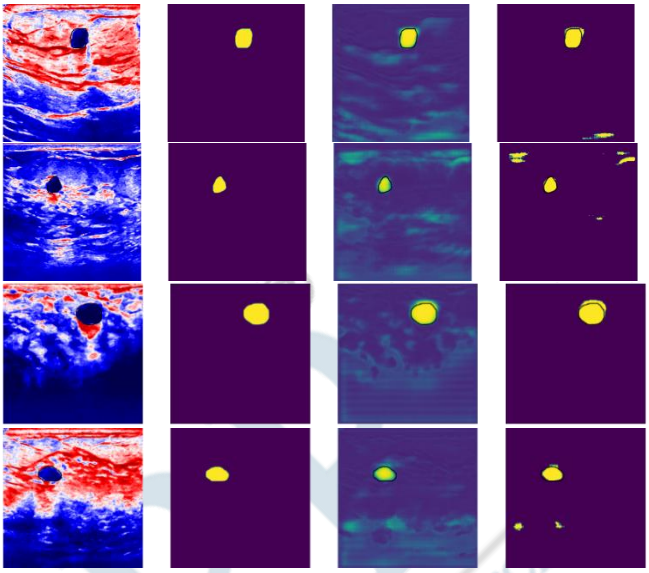

Fig. 6: Input Image, Ground Truth, Image Predicted, and Image Predicted Binary of the U-Net model

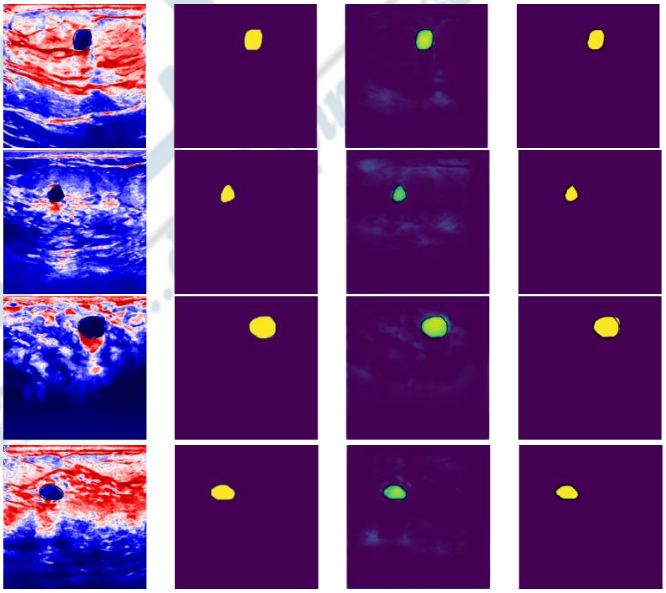

Fig. 7: Input Image, Ground Truth, Image Predicted, and Image Predicted Binary of the proposed ResUNet model for the same set of input images as in Fig. 6

Obviously, U-Net roughly distinguishes the lesions, but because of its complex structure, it is unable to accurately identify solely the targeted region. For instance, U-Net can easily misinterpret some lymph nodes and the surrounding tissue for lesions. The proposed ResUNet is able to comprehend the images from a variety of perspectives and offers better segmentation accuracy than the traditional U-Net, due to its powerful feature extraction capability.

Fig. 8 shows the plot of log loss, accuracy, dice coefficient and ROC curve during training and validation when using the dataset with ResUNet. Fig. 9(a) and Fig. 9(b) show that the proposed ResUNet model provides lesser loss and better accuracy respectively, in comparison with U-Net for both the

ISSN (Online) 2394-2320

International Journal of Engineering Research in Computer Science and Engineering (IJERCSE)

Vol 10, Issue 01, January 2023

training and validation phases. Fig. 9(c) shows the remarkable improvement of ResUNet for the values of DC over U-Net. The ROC with AUCs for U-Net and the proposed ResUNet are shown Fig. 9(d). In comparison with U-Net, the proposed ResUNet achieves a higher AUC. This eloquently underlines the reliability of the proposed ResUNet model in the overall image based semantic segmentation problems.

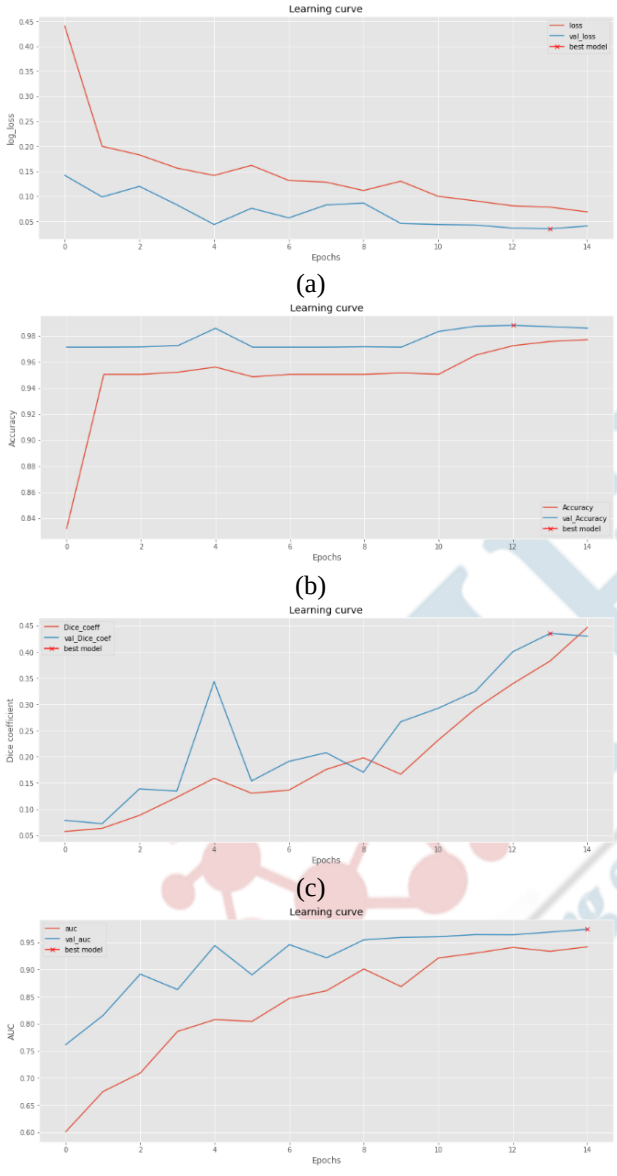

Fig 8: Plot of (a) loss, (b) accuracy, (c) dice coefficient and (d) ROC curve during training and validation when using the dataset with ResUNet

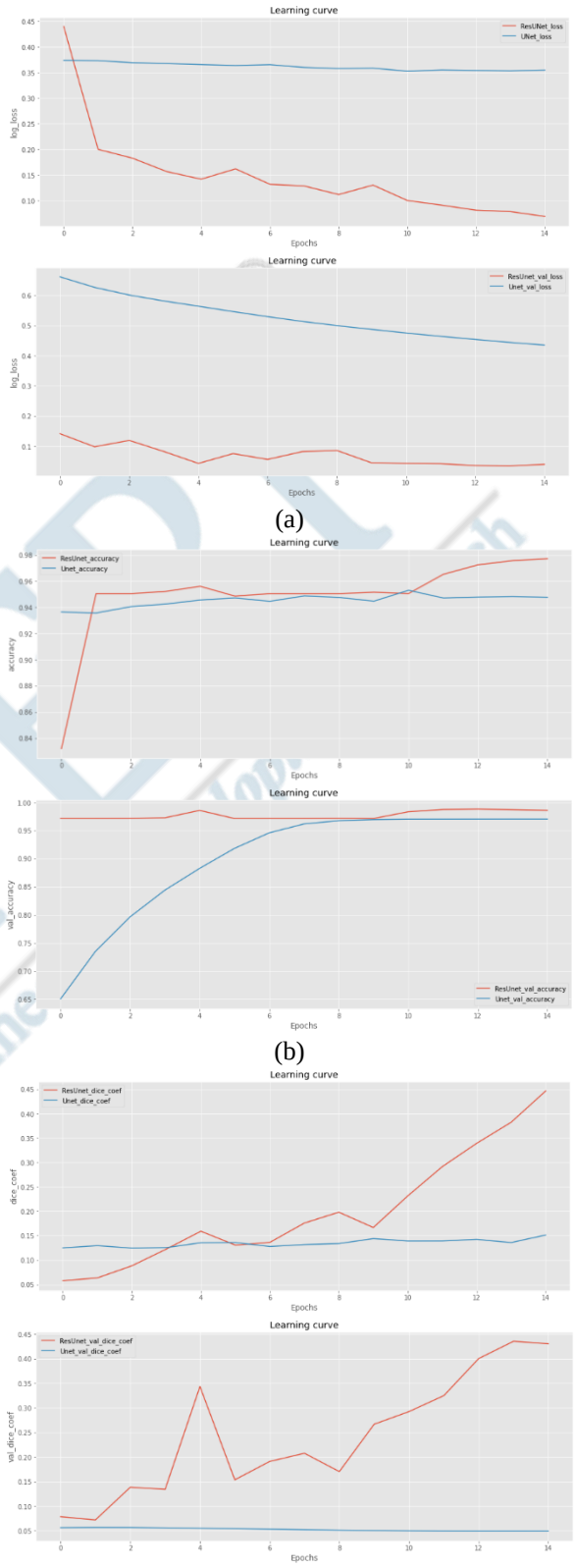

ISSN (Online) 2394-2320

International Journal of Engineering Research in Computer Science and Engineering (IJERCSE)

Vol 10, Issue 01, January 2023

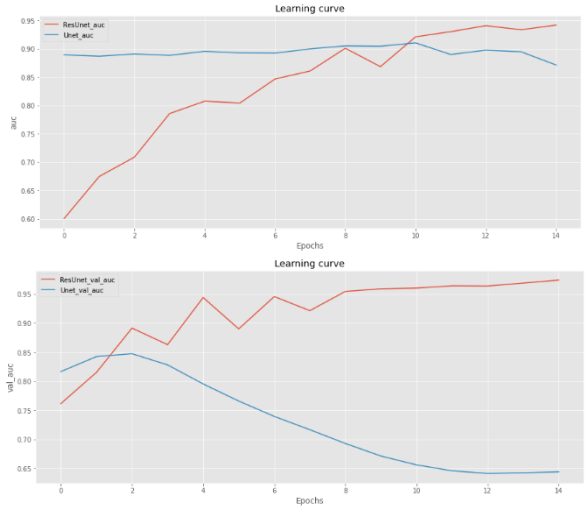

(d)

Fig. 9: Plot of (a) loss, (b) accuracy, (c) dice coefficient and (d) ROC curve during training and validation when using the dataset with ResUNet and U-Net.

V. CONCLUSION

In this modern era, people are prone to radioactive waves and avoid the consumption of healthy food, so the chances of developing a cancer are increasing exponentially.Severalprograms are being conducted to provide awareness about breast cancer and its symptoms, prevention, and therapies. One should maintain vigilance for the detection of breast cancer and consult their doctor if they notice any changes in their breasts, such as a new lump or skin changes. People can take certain measures to prevent this disease, such as limiting their alcohol consumption, maintaining a healthy weight and exercising regularly.

Breasts hold an important role in a woman's life. In some cases, during the treatment, they are advised to remove them, which affects their physical as well as mental health. So earlier stage precise detection is essential as the treatment process becomes much easier and the chances of survival also increase. In this case, accuracy is crucial because many cases go undetected. Therefore, in this paper we have proposed the ResUNet model which provides an accuracy of 0.9871 which is more than the accuracy of U-Net and similarly improves all other aspects in comparison with U-Net.

REFERENCES

[1] Kulothungan, V., Sathishkumar, K., Leburu, S., Ramamoorthy, T., Stephen, S., Basavarajappa, D., ... & Mathur, P. (2022). Burden of cancers in India-estimates of cancer crude incidence, YLLs, YLDs and DALYs for 2021 and 2025 based on National Cancer Registry Program. *BMC cancer*, *22*(1), 1-12.

[2] Mehrotra, R., & Yadav, K. (2022). Breast cancer in India: Present scenario and the challenges ahead. *World Journal of Clinical Oncology*, *13*(3), 209.

[3] Hesamian, M. H., Jia, W., He, X., & Kennedy, P. (2019). Deep learning techniques for medical image segmentation: achievements and challenges. *Journal of digital imaging*, *32*(4), 582-596.

[4] Inan, M. S. K., Alam, F. I., & Hasan, R. (2022). Deep integrated pipeline of segmentation guided classification of breast cancer from ultrasound images. *Biomedical Signal Processing and Control*, *75*, 103553.

[5] Tarighat, A. P. (2021). Breast Tumor Segmentation Using Deep Learning by U-Net Network. *Journal of Telecommunication, Electronic and Computer Engineering (JTEC)*, *13*(2), 49-54.

[6] Zhao, W., Lou, M., Qi, Y., Wang, Y., Xu, C., Deng, X., & Ma, Y. (2021). Adaptive channel and multiscale spatial context network for breast mass segmentation in full-field mammograms. *Applied Intelligence*, *51*(12), 8810-8827.

[7] Anand, I., Negi, H., Kumar, D., Mittal, M., Kim, T. H., & Roy, S. (2021). Residual U-Network for Breast Tumor Segmentation from Magnetic Resonance Images. *CMC-COMPUTERS MATERIALS & CONTINUA*, *67*(3), 3107-3127.

[8] Wu, H., Huo, Y., Pan, Y., Xu, Z., Huang, R., Xie, Y., ... & Wang, Y. (2022, July). Learning Pre-and Post-contrast Representation for Breast Cancer Segmentation in DCE-MRI. In *2022 IEEE 35th International Symposium on Computer-Based Medical Systems (CBMS)* (pp. 355-359). IEEE.

[9] Zhang, J., Li, C., Jiang, W., Wang, Z., Zhang, L., & Wang, X. (2022). Deep-learning-enabled Microwave-induced Thermoacoustic Tomography based on Sparse Data for Breast Cancer Detection. *IEEE Transactions on Antennas and Propagation*.

[10] Abdelhafiz, D., Nabavi, S., Ammar, R., Yang, C., & Bi, J. (2019, September). Residual deep learning system for mass segmentation and classification in mammography. In *Proceedings of the 10th ACM International Conference on Bioinformatics, Computational Biology and Health Informatics* (pp. 475-484).

[11] Al-Dhabyani W, Gomaa M, Khaled H, Fahmy A. Dataset of breast ultrasound images. Data in Brief. 2020 Feb; 28:104863. DOI: 10.1016/j.dib.2019.104863.

[12] Singhania, A., Narera, A., Rani, R., Dev, A., Bansal, P., & Sharma, A. (2022). Computer-aided Breast Cancer Diagnosis using Deep Convolutional Neural Networks. In 2022 International Conference on Computing, Communication, and Intelligent Systems (ICCCIS). IEEE. To be published.

[13] Xiao, X., Lian, S., Luo, Z., & Li, S. (2018, October). Weighted res-unet for high-quality retina vessel segmentation. In 2018 9th international conference on information technology in medicine and education (ITME) (pp. 327-331). IEEE.

[14] Li, X., Chen, H., Qi, X., Dou, Q., Fu, C. W., & Heng, P. A. (2018). H-DenseUNet: hybrid densely connected UNet for liver and tumor segmentation from CT volumes. IEEE transactions on medical imaging, 37(12), 2663-2674.

[15] He, K., Zhang, X., Ren, S., & Sun, J. (2016, October). Identity mappings in deep residual networks. In European conference on computer vision (pp. 630-645). Springer, Cham.

[16] Wang, F., Jiang, M., Qian, C., Yang, S., Li, C., Zhang, H., ... & Tang, X. (2017). Residual attention network for image classification. In Proceedings of the IEEE conference on computer vision and pattern recognition (pp. 3156-3164).

[17] Kingma, D. P., & Ba, J. (2014). Adam: A method for stochastic optimization. arXiv preprint arXiv:1412.6980.

[18] Dice, L. R. (1945). Measures of the amount of ecologic association between species. Ecology, 26(3), 297-302.